Substrate-Assisted Reductive Elimination Determining the Catalytic Cycle: Theoretical Study on the Ni-Catalyzed 2,3-Disubstituted Benzofurans Synthesis via C–O Bond Activation

Ray Miyazaki,[a] Kenji Iida,[b] Shohei Ohno,[c,‡] Tsuyoshi Matsuzaki,[d] Takeyuki Suzuki,[d] Mitsuhiro Arisawa,[c] and Jun-ya Hasegawa*[b]

[a] Fritz-Haber-Institut der Max-Planck-Gesellschaft, Faradayweg 4-6, D-14195 Berlin, Germany
[b] Institute for Catalysis, Hokkaido University, N21 W10 Kita-ku, Sapporo, Hokkaido 001-0021, Japan
[c] Graduate School of Pharmaceutical Sciences, Osaka University, Suita, Osaka 565-0871, Japan
[d] Comprehensive Analysis Centre, SANKEN (The Institute of Scientific and Industrial Research), Osaka University, Mihogaoka 8-1, Ibaraki, Osaka 567-0047, Japan
[‡] Present Address: Department of Chemistry, Yale University, New Haven, Connecticut 06520, United States

Abstract

The 2,3-disubstituted benzofurans with potential for pharmaceutical applications are effectively synthesized by Ni complexes via intramolecular C−O bond activation. The reaction pathway for the full catalytic cycle has been investigated by using density functional theory (DFT) calculations. The rate-determining step is the reductive elimination of the product. A key result is that coordination to alkynyl group of another substrate co-occurs with elimination, which not only improve thermodynamic stability of the product, but also determines the reaction pathway of the catalytic cycle. The reductive elimination assisted by the solvent molecules or free-ligand results in an endergonic reaction. This result is related to the enhancement of reductive elimination of C−C coupling products by the addition of olefin or alkyne, and can be recognized as a self-cocatalytic effect of the substrate. The result adds another view point in the design of catalytic reaction systems with effective catalytic cycles.

Table of contents

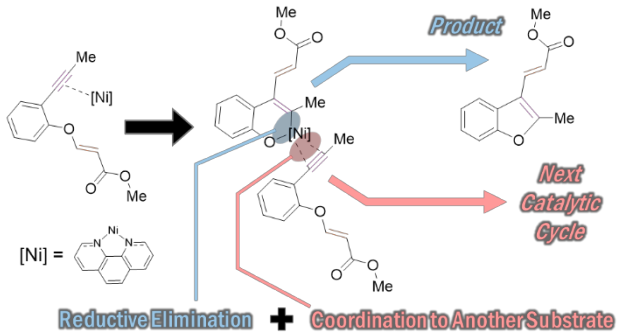

1. Introduction

The 2,3-disubstituted benzofuran skeletons present in numerous bioactive natural products and have a large potential for application to pharmaceuticals.[1-3] In 2019, we reported that Ni complexes effectively catalyze the synthesis of 2,3-disubstituted benzofurans via selective intramolecular C(vinyl)–O bond activation (Scheme 1).[4] This Ni complexes show high catalytic activity for a wide range of substituents at the 2- and 3-positions of benzofurans (e.g., silyl substituents).

Furthermore, as shown in Scheme 1, we also proposed a thermodynamically favorable reaction pathway based on the relative stabilities of the intermediates by using density functional theory (DFT) calculations.[4] The results showed that oxidative cyclization with alkynyl and vinyl groups (Path-A) was preferred over oxidative addition to the C(vinyl)–O bond (Path-B) because the corresponding intermediate, **Int A** in Path-A, was more stable than **Int B** in Path-B. However, transition states and activation energies were not discussed, and the rate-determining step was not identified in the previous report.[4] Therefore, the kinetically favorable pathway and full catalytic cycle remain unclear. Although several theoretical studies on C–O bond activation mechanisms by Ni complexes (e.g., C(phenyl)–O bond activation)[5-13] have been reported, theoretical studies on Ni-catalyzed C(vinyl)–O bond activation mechanisms are rather limited[14] to the best of our knowledge. In the present study, we thus investigated the full catalytic cycle in the synthesis of Ni-catalyzed 2,3-disubstituted benzofurans by using DFT calculations.

Scheme 1. Suggested reaction scheme for the synthesis of Ni-catalyzed 2,3-disubstituted benzofurans.[4] The ligand of the Ni complex (1,10-phenanthroline) is denoted as **L** in the structures of the intermediates. A comparison with our previous study is provided in S1 (Supporting Information, SI)

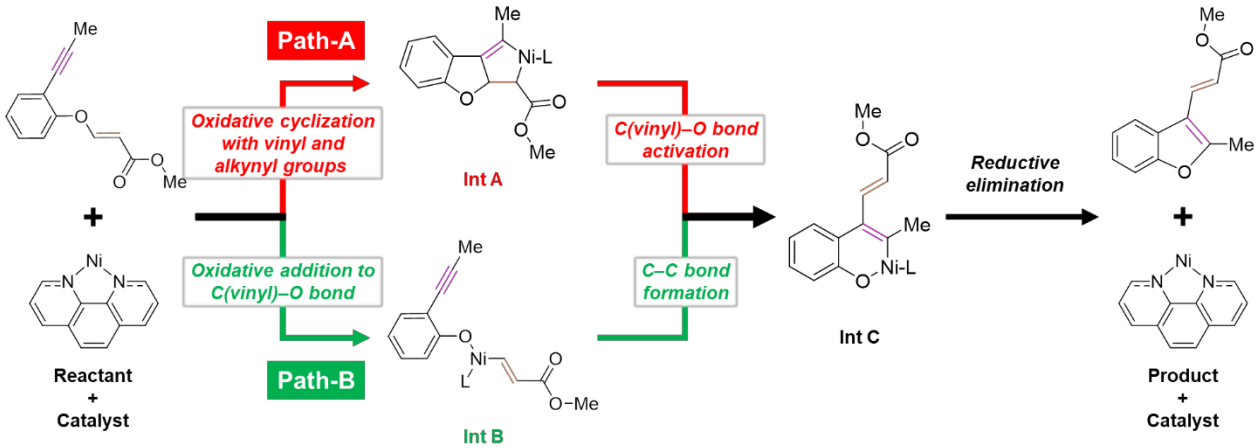

We particularly focused on the reductive elimination step from the final intermediate (i.e., **Int C** in Scheme 1). In a pioneering study by Komiya and Yamamoto,[15] Ni(II) catalysed C–O coupling reactions were accelerated by the addition of π–acid. Regarding C–C coupling, a comprehensive review was reported by

Rovis et al. about the effects of exogenous olefin and alkyne additives.[16] Yamamoto et al. reported that the reductive elimination and C−C coupling were promoted by olefin addition.[17] Tatsumi et al. proposed pentavalent Ni(II) intermediate.[18] The same intermediate was suggested for the C−O coupling case.[15] In recent years, electron deficient Fro-DO ligand was developed by Doyle et al. and applied to accelerate C−C cross coupling reactions.[19] A mechanistic study[20] showed that the Fro-DO binding to Ni(II) complex is thermodynamically stable, which is expected to continuously exert the trans effect which strongly promotes reductive elimination. According to Holland, alkyne binds more strongly to the metal center than olefin.[21]

Given these interesting results, it is worthwhile to investigate the role of the substrates with alkyne and olefine moieties in the reductive elimination step. In many of the DFT mechanistic investigations,[12] however, the product is simply eliminated from the catalyst. Thus, it would be natural to imagine that the catalyst in the elimination step is stabilized by the interaction with the next substrate, solvent molecules, even liberated ligand. In particular, if the product elimination is promoted by another substrate in a concerted manner, the elimination step directly connects to the next catalytic cycle. This would be recognized as a self-cocatalyst effect of the substrate. With this conjecture, we investigated such substrate-assisted reductive elimination mechanism. Additionally, the possibilities of the elimination mechanism assisted by the solvent molecules and uncoordinated ligand were also investigated for comparison.

2. Computational details

Electronic structure calculations were performed by Gaussian 16[22], and B3LYP functional[23, 24] with Grimme's D3 dispersion correction[25] was adopted for the approximated exchange-correlation functional of DFT. The Stuttgart/Dresden basis set with effective core potentials[26] was adopted for Ni, and the 6-31+G(d) basis set[27-29] was adopted for the other elements. The solvation effect of *N*,*N*-dimethylformamide (DMF) was incorporated by using the polarizable continuum model (PCM).[30] Geometry optimization for the equilibrium and transition states was performed by using GRRM 17.[31] The C=C and Ni−C bond lengths of $Ni(cod)_2$ were well represented by this calculation setting (deviation from the experimental value[32] is −0.005 Å for C=C bond and +0.025 Å for Ni−C bond). All reactants, products, and transition state structures were connected by intrinsic reaction coordinate (IRC) calculations. The Ni complex with the 1,10-phenanthroline (phen) ligand and intermediate states were calculated in the triplet state, and the other compounds (e.g., $Ni(cod)_2$, the reactant molecule, and so on) were calculated in the singlet state (see more details in S7 in SI). For **$Ni(phen)_2$**, which is assignable to Ni(0) triplet, the electronic structure is discussed in terms of orbital interactions between the Ni center and the phen ligands (S8 in SI).

Gibbs energy (G) was evaluated with a following equation.

$$G = E_{\mathrm{ele}} + E_{\mathrm{tra}} + E_{\mathrm{vib}} - T\left(S_{\mathrm{tra\_cor}} + S_{\mathrm{vib}}\right)$$

Where, E_{ele}, E_{vib}, and S_{vib} are electronic energy, vibrational energy, and vibrational entropy of a molecule in the PCM. E_{tra} is translational energy under the ideal gas approximation as adopted in the Gaussian program. $S_{\mathrm{tra\_cor}}$ is translational entropy in solution corrected by using the Whitesides scheme where the "free volume" of the molecule in solution was incorporated by taking account of volume and concentration of solvent molecules.[33] Although the Gaussian program adopts rotational energy of an ideal gas, the structure of the present system is very complex in solution, and the rotational motion should be suppressed by the interaction of the surrounding solvent molecules. Because of this reason, the rotational component in energy and entropy was neglected. In this study, the Gibbs free energy was calculated at T = 393.15 K that is the experimental temperature for the reaction.[4] Activation free energy ($\Delta G_{\mathrm{a}}^{\ddagger}$) and reaction free energy (ΔG_{r}) are defined as $\Delta G_{\mathrm{a}}^{\ddagger} = G_{\mathrm{TS}} - G_{\mathrm{R}}$ and $\Delta G_{\mathrm{r}} = G_{\mathrm{P}} - G_{\mathrm{R}}$, respectively, where G_{R}, G_{P}, and G_{TS} are Gibbs free energies of reactant, product, and transition states, respectively.

3. Results and discussion

3.1 Path-A via oxidative cyclization

The free energy profile of Path-A is illustrated in Figure 1, and the optimized structures of important intermediate and transition states along Path-A are shown in Figure 2. All the optimized structures are given in Figure S8 in SI.

To determine an appropriate reference structure for the relative energy, we investigated the relative stability of the Ni complexes before entering two catalytic pathways. As shown in Figure S10, **Ni(phen)$_2$** is the most stable Ni complex and has been set to the reference point with relative free energy of 0.0 kcal/mol. When one of the phen ligands is substituted by a substrate (methyl (E)-3-(2-(prop-1-yn-1-yl)phenoxy)acrylate), the precursor complex **IA2** for Path-A is formed. As seen in Figure 2a, the substrate in **IA2** is coordinated at the alkynyl group. The Ni−C(vinyl) distance was 3.05 Å, indicating the vinyl coordination to Ni is driven by van der Waals attractive interaction. After a minor energy barrier of 2.3 kcal/mol (**TSA2**), the vinyl group moves into η^2-coordinataion mode (**IA3**) where the Ni−C(vinyl) distances were 2.20 Å and 2.19 Å as shown in Figure 2b. This intermediate is a precursor to the cyclization with the vinyl and alkynyl groups. A five-membered metallacycle intermediate (**IA5**, Figure 2d) was formed via **TSA3** with energy barrier of $\Delta G_{\mathrm{aA3}}^{\ddagger} = 11.0$ kcal/mol (Figure 2c) from **IA3**. The activation energy from **Ni(phen)$_2$** was 16.9 kcal/mol. This **IA5** state corresponds to state **B** (see Scheme S1 in our previous report[4]) with terpyridine ligand and is by 23.4 kcal/mol more stable than the reference **Ni(phen)$_2$** state. As described in the later part of this manuscript, the relative energy of **IB4** state, which corresponds to state **A** (see Scheme S1 in our previous report[4]) is −15.1 kcal/mol. This result is consistent to our previous study, in which state **B** is by 8.5 kcal/mol more stable than state **A**.

Subsequently, C(vinyl)−O bond cleavage occurred (**TSA4**), and activation energy from **IA5** state was calculated to be 13.9 kcal/mol. The **TSA4** state relaxes to **IA7** state by rotating C_1–C_2 bond (see Figure 2e). The six-membered metalacyclic intermediate (**IA11**) was formed via O−Ni bond formation (**TSA5**, Figure 2f: $\Delta G^{\ddagger}_{\mathrm{aA5}} = 9.7$ kcal/mol from **IA7** state, 19.5 kcal/mol from **IA5** state) and C_2−Ni bond cleavage (**TSA6**, Figure 2g: $\Delta G^{\ddagger}_{\mathrm{aA6}} = 8.2$ kcal/mol from **IA10** state).

In the last step, reductive elimination of the product (methyl (E)-3-(2-methylbenzofuran-3-yl)acrylate) occurs, and this step was calculated to be the rate-determining step of Path-A ($\Delta G^{\ddagger}_{\mathrm{aA7}} = 27.9$ kcal/mol from **IA12**). In this step, coordination to the alkynyl group of another substrate takes place (**IA12**, Figure 2h) prior to the reductive elimination (**TSA7**, Figure 2i). In the **IA12** state, the new substrate coordinates to the Ni center at the alkynyl group with the Ni−C distance of 3.5 Å. This complexation would be led not only by the alkynyl coordination but also other interaction such as π–π stacking and dispersion forces. In the transition state, the Ni−C distance becomes shorter with promoting the elimination of the product in a concerted manner. The Ni−O distance in the **TSA7** state is by 0.15 Å longer than that in the **IA12** state as seen in Figures 2h and 2i. In the product state (**IA13**), the coordination of the substrate completed, and the reductive elimination also completed in a concerted manner. The reaction free energy of this step was calculated to be −5.2 kcal/mol. After the product leaves the catalyst-substrate complex, this **IA13** state becomes equivalent to the **IA2** state. This means that the reductive elimination connects with the next catalytic cycle by returning back to the **IA2** state as an exergonic reaction.

On the other hand, the activation energy for the reductive elimination without another substrate was calculated to be 28.8 kcal/mol, and this process is an endergonic reaction ($\Delta G_{\mathrm{r}} = +7.1$ kcal/mol: see Table 1 and S2 in SI). In the experimental reactor, substrate molecules are in the surroundings. Thus, this substrate-assisted reductive elimination, which makes direct connection to the next catalytic cycle, are more plausible than a stepwise mechanism via the elimination followed by the coordination of the next substrate.

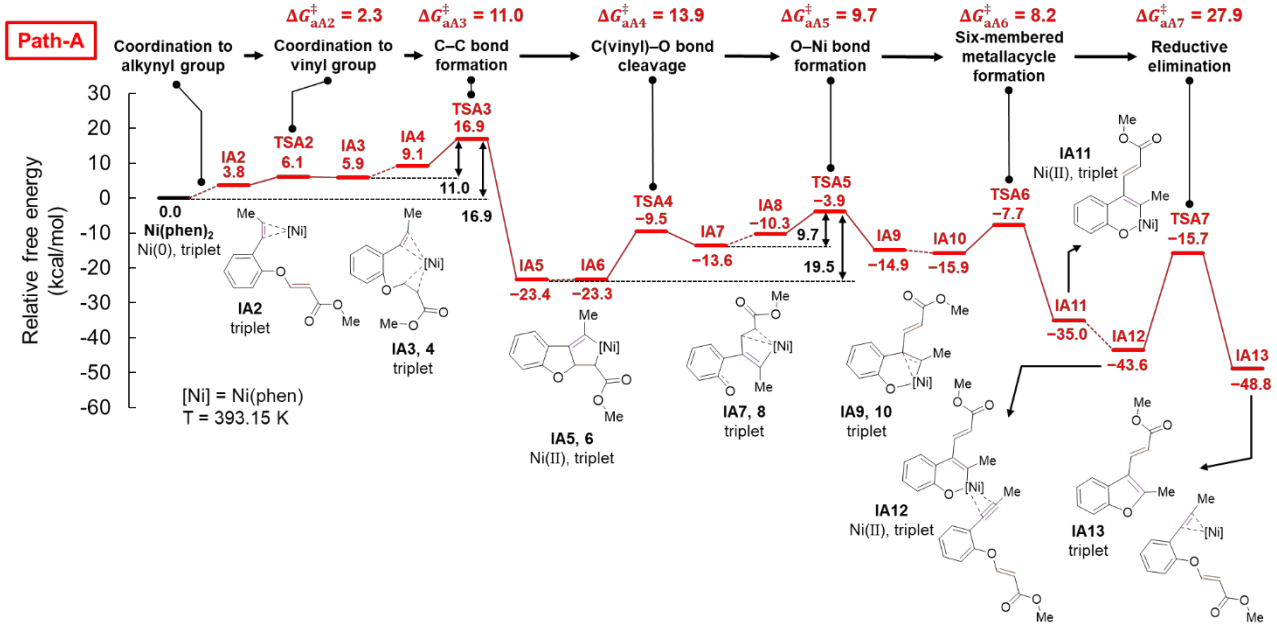

Figure 1. Free energy profiles of Path-A. The phenanthroline ligand (phen) of the catalyst is not visualized for simplicity. The detail of the electronic structure of Ni in key intermediates is discussed in S7 and S8 in SI.

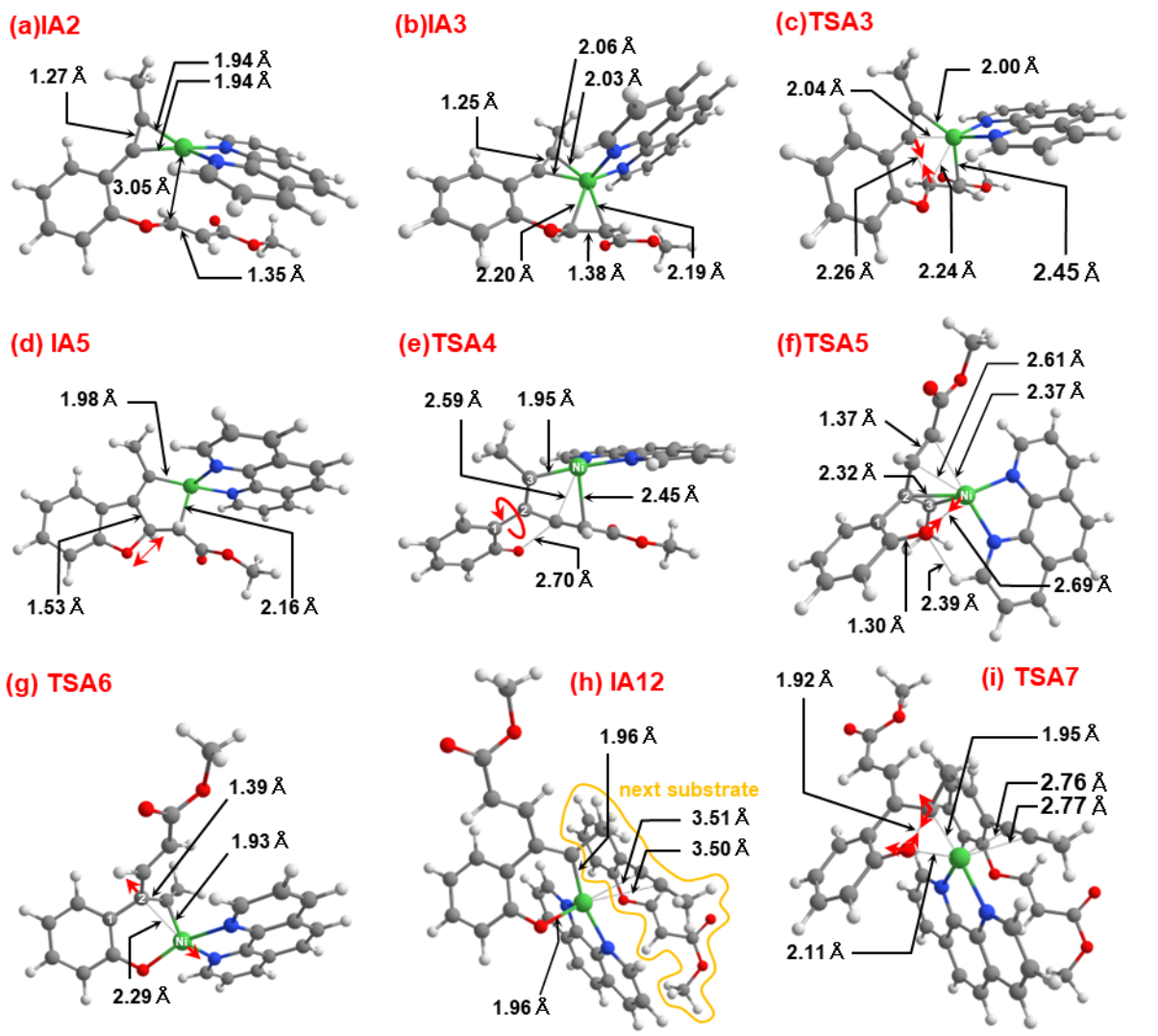

Figure 2. Some important intermediate and transition state structures along Path-A. White: hydrogen, gray: carbon, red: oxygen, green: nickel, and blue: nitrogen. Red arrows indicate bond rotations, formations, and cleavages. All the optimized structures were shown in Figure S8 in SI.

Because the intermediate is also surrounded by solvent molecules and uncoordinated ligands in the reactor, we also investigated the reductive elimination mechanism with the explicit solvent molecules (solvent-assisted reductive elimination) or uncoordinated ligand (free ligand-assisted reductive elimination), which might stabilize the elimination process. As shown in Table 1, the activation energies of the solvent-assisted mechanisms are lower than that without assistance and the substrate-assisted mechanisms (see also Figure S2 in SI). However, those pathways were calculated to be endergonic reactions ($\Delta G_{\mathrm{r}} =$ +6.3 and +14.1 kcal/mol with one and two explicit DMF molecules, respectively), indicating that the reductive elimination with DMF molecules is thermodynamically unfavorable than the substrate-assisted mechanism. Regarding the free ligand-assisted mechanism, activation energy is only 0.2 kcal/mol lower than that of the substrate-assisted mechanism (see also Figure S3). The reaction energy was, however,

calculated to be +6.0 kcal/mol, and the elimination with the uncoordinated phenanthroline ligand thus proceeds as an endergonic reaction.

Table 1. Activation and reaction free energies for the direct, solvent-assisted, and free ligand-assisted reductive elimination mechanisms.

parameters (T = 393.15 K)	substrate-assisted		w/o assistance	solvent-assisted		free ligand-assisted
	alkynyl coordination	carbonyl coordination		with 1 DMF	with 2 DMF	
$\Delta G_a^{\ddagger}$ (kcal/mol)	27.9	28.0	28.8	25.3	23.6	27.7
ΔG_r (kcal/mol)	−5.2	+9.7	+7.1	+6.3	+14.1	+6.0

The driving force for the exergonicity is in the stability of the alkynyl−Ni η^2-coordinataion. Related phenomena were reported in previous studies, showing that olefin ligands promote reductive elimination.[16-21]

3.2 Role of alkynyl group for promoting reductive elimination

Thermodynamic stability of the reductive elimination step was compared in several examples as shown in Table 1. Among them, only the case of alkynyl coordination was thermodynamically favored. This is consistent with the previous result that only the Fro-DO ligand has dG < 0 [20] and that alkyne is more strongly complexed than olefin [21]. On the other hand, because of the structural complexity, the alkyne moiety was not strongly bound to Ni center at the beginning of the complex formation. As shown in Figure 2h, the optimized Ni−C distance was 3.5 Å, indicating physisorption. The alkyne moiety, however, coordinated to the oxygen atom of product in the trans position, suggesting that the trans effect of alkyne would affect thermodynamic stability.

The result in Table 1 showed that the assistance with solvent molecules and the free ligand leads thermodynamically unstable product state, which would move back to the initial state before the elimination. Additionally, in those mechanisms, further reaction steps and activation energies for the elimination of DMF or ligand are required to proceed to the next catalytic cycle. Therefore, a stable complex formation with new substrate is an important factor not only to complete the single catalytic cycle but also to effectively connect to the early stage of the next catalytic cycle.

It is worth mentioning that the alkyne moiety in the substrate, which promotes the reductive elimination, is not an additive as in previous examples,[15-17, 19] but a part of the substrate. This is a unique characteristic of the present catalytic reaction system. The additive moiety coordinates to Ni(II) center when necessary and does not inhibit other reaction steps as a part of substrate.

3.3 Path-B via oxidative addition to C(vinyl)–O bond

A free energy profile of Path-B is illustrated in Figure 3, and optimized structures of important equilibrium and transition states are shown in Figure 4. All the optimized structures are also given in Figure S9 in SI. **Ni(phen)$_2$** undergoes a ligand exchange by a substrate, and **IB1** is formed (see Figure S10). The substrate makes a η^2-complex with the Ni catalyst at the vinyl group (see Figure 4a). After a minor structural change to **IB2**, the Ni complex undergoes oxidative addition to the C(vinyl)–O bond (**TSB2**, Figure 4b, $\Delta G^{\ddagger}_{\mathrm{aB2}} = 16.5$ kcal/mol). This TS is the highest energy structure in the energy profile, and the apparent activation barrier from **Ni(phen)$_2$** is 29.1 kcal/mol. Because of the barrier height, the reaction from **Ni(phen)$_2$** should enter into Path-A. After C–C bond formation between the vinyl and alkynyl groups (**TSB3**, Figure 4c, $\Delta G^{\ddagger}_{\mathrm{aB3}} = 27.3$ kcal/mol), the α,β-unsaturated methyl ester group (–CH=CH–COOMe) is transferred to alkynyl group (**IB6** , Figure 4d), keeping the η^2-coordination to Ni center. A six-membered metalacyclic intermediate (**IB7**, Figure 4f) was formed via **TSB4** (Figure 4e, $\Delta G^{\ddagger}_{\mathrm{aB4}} = 6.5$ kcal/mol). This **IB7** is structurally equivalent to the **IA11** intermediate in Path-A. The Ni–O and Ni–C bond lengths in **IB7** are 1.92 Å and 1.98 Å, respectively, while those in **IA11** were 1.90 Å and 1.97 Å, respectively. A dihedral angle C–Ni–N–C of **IB7**, an angle between the newly formed 6 membered metallacycle and phenanthroline ligand (see Figure 4f), is 101.0 degrees, while that of **IA11** is 100.1 degrees. This similarity implies that the Path-B is connected to Path-A at the **IB7** intermediate. The reductive elimination step plays as a switching role and connects **IB7** to either **IA2** in Path-A or **IB1** in Path-B.

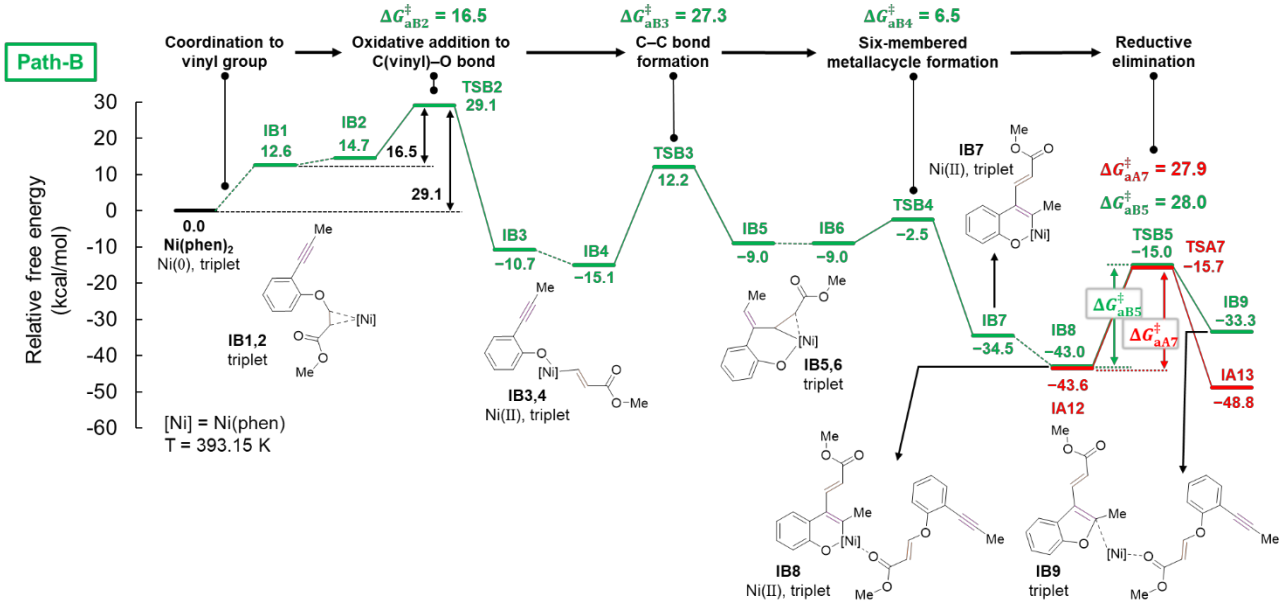

Figure 3. Free energy profiles of Path-B. In this figure, the ligand of the catalyst is not visualized for simplicity. The detail of the electronic structure of Ni in key intermediates is discussed in S7 and S8 in SI.

According to the result of Path-A, the substrate-assisted reductive elimination was also assumed for Path-B. To restart catalytic cycle via **IB1**, the next substrate should coordinate to **IB7** at the vinyl group in a

η^2-mode, and the reductive elimination happens sequentially. However, this vinyl coordination to **IB7** requires the benzene ring of the substrate to be on the same plane as the vinyl group to minimize the steric repulsion with the **IB7** intermediate. As a result, the new substrate coordinates at the carboxyl O atom in the ester group as illustrated in **IB8**, Figure 4g. This complexation would also be led by dispersion forces. The obtained transition state (**TSB5**, Figure 4h) is connected to a product state (**IB9**, Figure 4i) keeping the interaction with the O atom (Ni−O distance = 3.5 Å). This elimination needs to go over one of the highest energy barriers ($\Delta G^{\ddagger}_{\mathrm{aB5}} = 28.0$ kcal/mol) and also is an endergonic reaction ($\Delta G_{\mathrm{r}} = +9.7$ kcal/mol). As a result, the pathway back to **IB1** of Path-B could be closed at this step. Conversely, **IB7** is also connected to **IA12** of Path-A after another substrate coordinates to the alkynyl group. Thus, the plausible reaction pathway is able to switch into Path-A by the preferable coordination mode of the next substrate. In the experimental side, NMR and mass spectrometry measurements were conducted to observe intermediates. We only observed starting material and product by NMR analysis, while mass spectrometry results gave some information of the reaction intermediates (see S4 in SI). The calculated results are not conflicted with the experimental results.

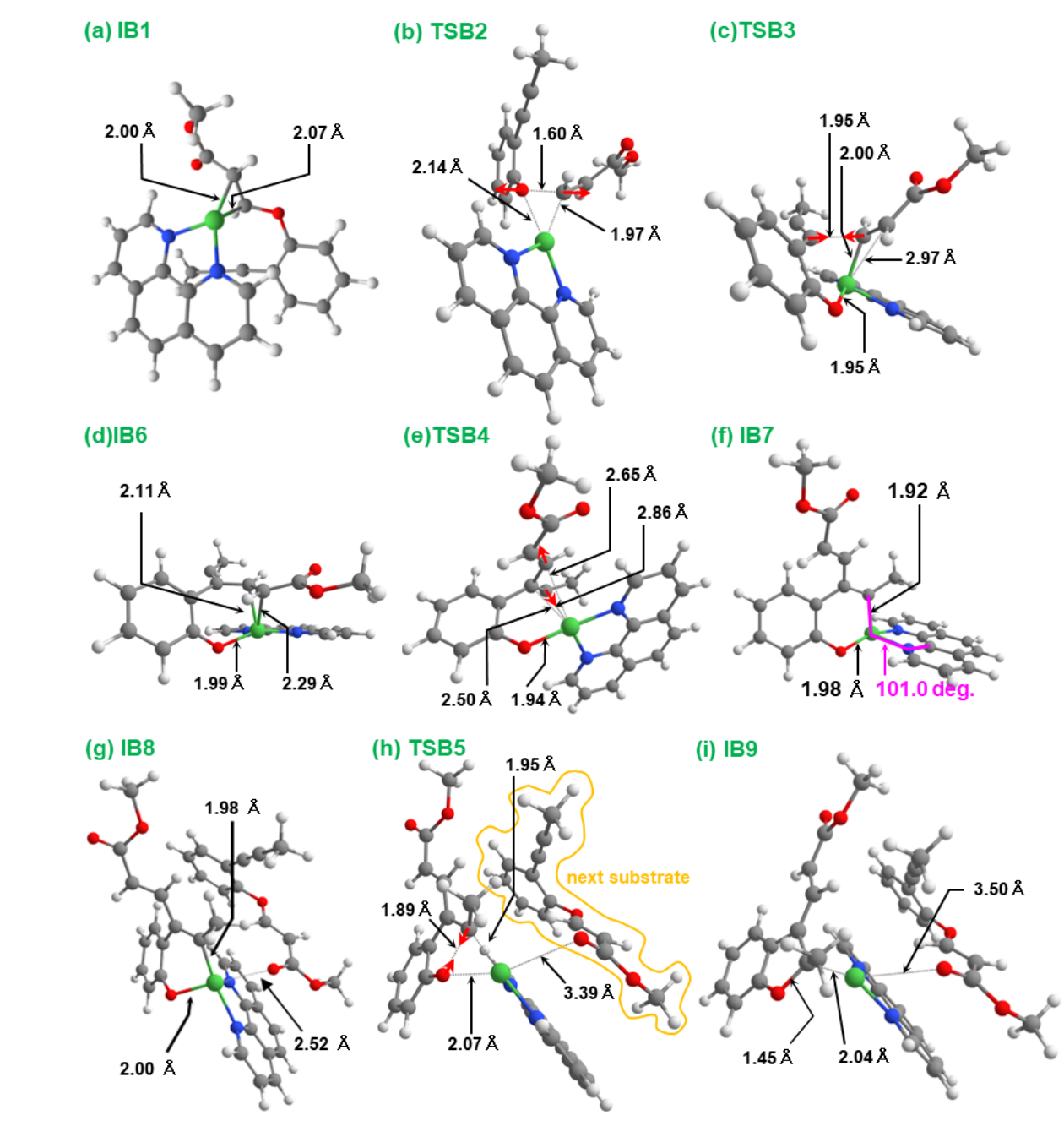

Figure 4. Equilibrium and transition state structures along Path-B. White: hydrogen, gray: carbon, red: oxygen, green: nickel, and blue: nitrogen. Red arrows indicate bond formations and cleavages. All the optimized structures were also shown in Figure S9 in SI.

4. Conclusions

The full catalytic cycle for the Ni-catalyzed synthesis of 2,3-disubstituted benzofuran was investigated by using DFT calculations. We focused on two pathways as shown in Scheme 1, oxidative cyclization initiated by the coordination to the alkynyl group (Path-A) and oxidative addition to the C(vinyl)–O bond (Path-B). Starting with the most stable **Ni(phen)$_2$**, Path-A should be selected because Path-B should go over the

highest activation barrier of 29.1 kcal/mol for oxidative addition of C(vinyl)-O bond. The rate-determining step of Path-A is the reductive elimination from the final intermediate state with the activation energy of 27.9 kcal/mol. Even if the reaction takes place via Path-B, this elimination step appears in the end of the pathway. In this step, coordination to the alkynyl group of another substrate co-occurred with reductive elimination, and the catalytic cycle was smoothly connected to Path-A, even from Path-B. This substrate-assisted reductive elimination mechanism is kinetically and thermodynamically preferred over the stepwise mechanism, which involves direct elimination prior to coordination to the next substrate. Although the reductive elimination would also be assisted by solvent molecules and free ligand, these eliminations were calculated to be endergonic processes. The result indicates that the relatively stable coordination of a new substrate should be a key aspect not only to complete the single catalytic cycle but also to effectively connect to the early stage of the next catalytic cycle.

In previous pioneering studies,[15-17, 19] C–C cross coupling reactions by Ni(II) catalysts have been reported to be enhanced by the addition of olefins or alkynes. The present study indicates that the reductive C–O coupling by Ni(II) catalysts can be similarly promoted by coordinating the substrate at the alkyne moiety. This is an especially unique characteristic of the present catalytic reaction system in that the substrate also plays as a self-cocatalyst. The present study would add another viewpoint in the design of an effective catalytic cycle.

Associated Content

Supporting Information-1

Computational settings, Reductive elimination without another substrate, Reductive elimination with DMF molecules or another ligand, Experimental results of mass spectrometry, Energy levels of the Ni complex before entering Paths-A and B, Comparison between singlet and triplet states of the key intermediates, and Detail of the electronic structure of $Ni(phen)_2$.

Supporting Information-2

Cartesian coordinates of optimized structures in the ".xyz" format.

Author Information

Corresponding Author

Jun-ya Hasegawa

*hasegawa@cat.hokudai.ac.jp

Conflicts of interest

There are no conflicts to declare.

Acknowledgements

This work was financially supported by JSPS KAKENHI Grant Numbers 15H05805 and 20H02685. This study was supported by the Cooperative Research Program of the Institute for Catalysis, Hokkaido University (Proposal#19B1019, 20A1006 and 21B1028). This study was also supported by the Photoexcitonix Project at Hokkaido University and the MEXT project "Integrating Research Consortium on Chemical Science." The computation was performed using Research Center for Computational Science, Okazaki, Japan (Project: 22-IMS-C002). R.M. acknowledges the Max Planck research network on big-data-driven materials science (BiGmax) for financial support.

References

1. Goyal, D.; Kaur, A.; Goyal, B., Benzofuran and Indole: Promising Scaffolds for Drug Development in Alzheimer's Disease. *ChemMedChem* **2018,** *13*, 1275-1299.
2. Heravi, Majid M.; Zadsirjan, V.; Hamidi, H.; Tabar Amiri, P. H., Total synthesis of natural products containing benzofuran rings. *RSC Adv.* **2017,** *7*, 24470-24521.
3. Hiremathad, A.; Patil, M. R.; K. R, C.; Chand, K.; Santos, M. A.; Keri, R. S., Benzofuran: an emerging scaffold for antimicrobial agents. *RSC Adv.* **2015,** *5*, 96809-96828.
4. Ohno, S.; Qiu, J.; Miyazaki, R.; Aoyama, H.; Murai, K.; Hasegawa, J.; Arisawa, M., Ni-Catalyzed Cycloisomerization between 3-Phenoxy Acrylic Acid Derivatives and Alkynes via Intramolecular Cleavage and Formation of the C–O Bond To Give 2,3-Disubstituted Benzofurans. *Org. Lett.* **2019,** *21*, 8400-8403.
5. Doi, R.; Shimizu, K.; Ikemoto, Y.; Uchiyama, M.; Koshiba, M.; Furukawa, A.; Maenaka, K.; Watanabe, S.; Sato, Y., Nickel-Catalyzed Acyl Group Transfer of *o*-Alkynylphenol Esters Accompanied by C–O Bond Fission for Synthesis of Benzo[*b*]furan. *ChemCatChem* **2021,** *13*, 2086-2092.
6. Yang, Z.-K.; Wang, C.; Uchiyama, M., DFT Studies Provide Mechanistic Insight into Nickel-Catalyzed Cross-Coupling Involving Organoaluminum-Mediated C–O Bond Cleavage. *Synlett* **2017,** *28*, 2565-2568.
7. Kojima, K.; Yang, Z.-K.; Wang, C.; Uchiyama, M., Ethereal C–O Bond Cleavage Mediated by Ni(0)-Ate Complex: A DFT Study. *Chem. Pharm. Bull.* **2017,** *65*, 862-868.

8. Ogawa, H.; Minami, H.; Ozaki, T.; Komagawa, S.; Wang, C.; Uchiyama, M., How and Why Does Ni^0 Promote Smooth Etheric C−O Bond Cleavage and C−C Bond Formation? A Theoretical Study. *Chem. Eur. J.* **2015,** *21*, 13904-13908.
9. Li, X.; Hong, X., Computational studies on Ni-catalyzed C−O bond activation of esters. *J. Organomet. Chem.* **2018,** *864*, 68-80.
10.Hong, X.; Liang, Y.; Houk, K. N., Mechanisms and Origins of Switchable Chemoselectivity of Ni-Catalyzed C(aryl)–O and C(acyl)–O Activation of Aryl Esters with Phosphine Ligands. *J. Am. Chem. Soc.* **2014,** *136*, 2017-2025.
11.Li, Z.; Zhang, S.-L.; Fu, Y.; Guo, Q.-X.; Liu, L., Mechanism of Ni-Catalyzed Selective C−O Bond Activation in Cross-Coupling of Aryl Esters. *J. Am. Chem. Soc.* **2009,** *131*, 8815-8823.
12.Sperger, T.; Sanhueza, I. A.; Kalvet, I.; Schoenebeck, F., Computational Studies of Synthetically Relevant Homogeneous Organometallic Catalysis Involving Ni, Pd, Ir, and Rh: An Overview of Commonly Employed DFT Methods and Mechanistic Insights. *Chem. Rev.* **2015,** *115*, 9532-9586.
13.Tobisu, M.; Chatani, N., Cross-Couplings Using Aryl Ethers via C–O Bond Activation Enabled by Nickel Catalysts. *Acc. Chem. Res.* **2015,** *48*, 1717-1726.
14.Iqbal, N.; Lee, D. S.; Jung, H.; Cho, E. J., Synergistic Effects of Boron and Oxygen Interaction Enabling Nickel-Catalyzed Exogenous Base-Free Stereoselective Arylvinylation of Alkynes through Vinyl Transposition. *ACS Catal.* **2021,** *11*, 5017-5025.
15.Komiya, S.; Akai, Y.; Tanaka, K.; Yamamoto, T.; Yamamoto, A., Reductive elimination of aryl carboxylates from acyl(aryloxy)nickel(II) and -palladium(II) complexes. *Organometallics* **1985,** *4*, 1130-1136.
16.Johnson, J. B.; Rovis, T., More than bystanders: The effect of Olefins on transition-metal-catalyzed cross-coupling reactions. *Angewandte Chemie-International Edition* **2008,** *47*, 840-871.
17.Yamamoto, T.; Yamamoto, A.; Ikeda, S., Organo (dipyridyl) nickel complexes. I. Stability and activation of the alkyl-nickel bonds of dialkyl (dipyridyl) nickel by coordination with various substituted olefins. *J Am Chem Soc* **1971,** *93*, 3350-3359.
18.Tatsumi, K.; Nakamura, A.; Komiya, S.; Yamamoto, A.; Yamamoto, T., An Associative Mechanism for Reductive Elimination of D8 Nir2(Pr3)2. *J Am Chem Soc* **1984,** *106*, 8181-8188.
19.Huang, C.-Y.; Doyle, A. G., Electron-Deficient Olefin Ligands Enable Generation of Quaternary Carbons by Ni-Catalyzed Cross-Coupling. *J Am Chem Soc* **2015,** *137*, 5638-5641.
20.Estrada, J. G.; Williams, W. L.; Ting, S. I.; Doyle, A. G., Role of Electron-Deficient Olefin Ligands in a Ni-Catalyzed Aziridine Cross-Coupling To Generate Quaternary Carbons. *J Am Chem Soc* **2020,** *142*, 8928-8937.
21.Yu, Y.; Smith, J. M.; Flaschenriem, C. J.; Holland, P. L., Binding Affinity of Alkynes and Alkenes to Low-Coordinate Iron. *Inorg Chem* **2006,** *45*, 5742-5751.
22.Frisch, M. J.; Trucks, G. W.; Schlegel, H. B.; Scuseria, G. E.; Robb, M. A.; Cheeseman, J. R.; Scalmani, G.; Barone, V.; Petersson, G. A.; Nakatsuji, H.; Li, X.; Caricato, M.; Marenich, A. V.; Bloino, J.; Janesko, B. G.; Gomperts, R.; Mennucci, B.; Hratchian, H. P.; Ortiz, J. V.; Izmaylov, A. F.; Sonnenberg, J. L.; Williams; Ding, F.; Lipparini, F.; Egidi, F.; Goings, J.; Peng, B.; Petrone, A.; Henderson, T.; Ranasinghe, D.; Zakrzewski, V. G.; Gao, J.; Rega, N.; Zheng, G.; Liang, W.; Hada, M.; Ehara, M.; Toyota, K.; Fukuda, R.; Hasegawa, J.; Ishida, M.; Nakajima, T.; Honda, Y.; Kitao, O.; Nakai, H.; Vreven, T.; Throssell, K.; Montgomery Jr., J. A.; Peralta, J. E.; Ogliaro, F.; Bearpark, M. J.; Heyd, J. J.; Brothers, E. N.; Kudin, K. N.; Staroverov, V. N.; Keith, T. A.; Kobayashi, R.; Normand, J.; Raghavachari, K.; Rendell, A. P.; Burant, J. C.; Iyengar, S. S.; Tomasi, J.; Cossi, M.; Millam, J. M.; Klene, M.; Adamo, C.; Cammi, R.; Ochterski, J. W.; Martin, R. L.; Morokuma, K.; Farkas, O.; Foresman, J. B.; Fox, D. J., *Gaussian 16 Rev. C.01, Wallingford, CT* **2016**.
23.Becke, A. D., Density‐functional thermochemistry. III. The role of exact exchange. *J. Chem. Phys.* **1993,** *98*, 5648-5652.
24.Lee, C.; Yang, W.; Parr, R. G., Development of the Colle-Salvetti correlation-energy formula into a functional of the electron density. *Phys. Rev. B* **1988,** *37*, 785-789.
25.Grimme, S.; Antony, J.; Ehrlich, S.; Krieg, H., A consistent and accurate ab initio parametrization of density functional dispersion correction (DFT-D) for the 94 elements H-Pu. *J. Chem. Phys.* **2010,** *132*, 154104.
26.Dolg, M.; Wedig, U.; Stoll, H.; Preuss, H., Energy‐adjusted ab initio pseudopotentials for the first row transition elements. *J. Chem. Phys.* **1987,** *86*, 866-872.
27.Frisch, M. J.; Pople, J. A.; Binkley, J. S., Self‐consistent molecular orbital methods 25. Supplementary functions for Gaussian basis sets. *J. Chem. Phys.* **1984,** *80*, 3265-3269.

28.Hariharan, P. C.; Pople, J. A., The influence of polarization functions on molecular orbital hydrogenation energies. *Theoret. Chim. Acta* **1973,** *28*, 213-222.
29.Hehre, W. J.; Ditchfield, R.; Pople, J. A., Self—Consistent Molecular Orbital Methods. XII. Further Extensions of Gaussian—Type Basis Sets for Use in Molecular Orbital Studies of Organic Molecules. *J. Chem. Phys.* **1972,** *56*, 2257-2261.
30.Tomasi, J.; Mennucci, B.; Cammi, R., Quantum Mechanical Continuum Solvation Models. *Chem. Rev.* **2005,** *105*, 2999-3094.
31.Maeda, S.; Ohno, K.; Morokuma, K., Systematic exploration of the mechanism of chemical reactions: the global reaction route mapping (GRRM) strategy using the ADDF and AFIR methods. *Phys. Chem. Chem. Phys.* **2013,** *15*, 3683-3701.
32.Macchi, P.; Proserpio, D. M.; Sironi, A., Experimental Electron Density Studies for Investigating the Metal π-Ligand Bond: the Case of Bis(1,5-cyclooctadiene)nickel. *J. Am. Chem. Soc.* **1998,** *120*, 1447-1455.
33.Mammen, M.; Shakhnovich, E. I.; Deutch, J. M.; Whitesides, G. M., Estimating the Entropic Cost of Self-Assembly of Multiparticle Hydrogen-Bonded Aggregates Based on the Cyanuric Acid·Melamine Lattice. *The Journal of Organic Chemistry* **1998,** *63*, 3821-3830.